Macromolecules
ARTICLE

Macromolecules **2009**, *42*, 8485–8491 **8485**
DOI: 10.1021/ma901661d

Anomaly in Stretching-Induced Swelling of Slide-Ring Gels with Movable Cross-Links

Naoki Murata,[†] Akihiro Konda,[†] Kenji Urayama,*[,†] Toshikazu Takigawa,[†] Masatoshi Kidowaki,[‡,§] and Kohzo Ito*[,‡]

[†]*Department of Materials Chemistry, Kyoto University, Nishikyo-ku, Kyoto 615-8510, Japan, and* [‡]*Graduate School of Frontier Sciences, The University of Tokyo, 5-1-5 Kashiwanoha, Kashiwa 277-8561, Japan.* [§] *Present address: Department of Applied Chemistry, Shibaura Institute of Technology, 3-7-5 Toyosu, Koto-ku, Tokyo 135-8548, Japan*

Received July 28, 2009; Revised Manuscript Received September 3, 2009

ABSTRACT: Stretching-induced swelling is investigated for polyrotaxane (PR)-based slide-ring gels with movable cross-links. The osmotic Poisson's ratio (μ_{os}), which is a measure of strain-induced swelling, is examined as a function of imposed stretching (α_x) for three types of PR gels with various degrees of the mobility of slide-rings. Classical gels with topologically fixed cross-links and PR gels with constrained slide-rings exhibit α_x-independent μ_{os}. In contrast, PR gels with highly mobile slide-rings exhibit α_x-dependent μ_{os}. The μ_{os} increases with α_x in the case of moderate stretching ($\alpha_x < 1.5$), whereas it levels off in the case of high stretching ($\alpha_x > 1.5$). An increase in μ_{os} with elongation results from the molecular pulley effect of slide-rings that homogenizes the structure of deformed networks. The pulley effect suppresses the stretching-induced swelling that originates from an entropic force to reduce the configurational anisotropy of the deformed networks.

Introduction

Slide-ring (SR) gels have received considerable attention as a novel type of polymer gel whose cross-links are movable along the network strands, in contrast to the topologically fixed cross-links of classical gels.[1,2] The network chains in SR gels are topologically interlocked by figure-of-eight cross-links (slide-rings). The movable cross-links are expected to act like pulleys when the gels deform. These cross-links slide along the network strands so that the configurational entropy of the networks can be maximized; i.e., the resultant entropic force can be minimized. This "pulley effect" is a property unparalleled in polymer gels. Okumura and Ito[3] first synthesized polyrotaxane (PR)-based SR gels by the intermolecular cross-linking of α-cyclodextrin (α-CD) contained in poly(ethylene glycol) (PEG).

The unique features of the microscopic structure of SR gels have been revealed by small-angle neutron[4] or X-ray[5] scattering experiments. The scattering intensity of the uniaxially stretched SR gels showed the so-called "normal butterfly pattern" (i.e., prolate pattern perpendicular to the stretching axis)[4] or almost isotropic pattern,[5] both of which are substantially different from the abnormal butterfly pattern (prolate pattern parallel to the stretching axis) observed in the stretched classical gels with fixed cross-links.[6−8] The abnormal butterfly pattern in the classical gels originates from frozen inhomogeneity due to the nonuniform distribution of cross-links.[9,10] The scattering data of the stretched SR gels indicate the presence of the pulley effect that homogenizes the network topology under imposed deformation.[4,5]

SR gels with pulley effects exhibit intriguing macroscopic properties such as high extensibility and marked swellability in solvents.[2,3] Several researchers have studied the dynamic mechanical properties of SR gels under sinusoidal oscillation of a small strain,[11,12] and in some cases, the relaxation characteristic of the movable cross-links was observed.[11] The present study focuses on the stretching-driven swelling of SR gels under finite elongation. It is known that gels that are fully swollen in solvents change their volume when a constant strain is imposed externally. Thus, the extensional strain drives further swelling,[13,14] while the compressive strain induces deswelling.[15] Several theoretical models have been proposed to describe the strain-induced volume change in gels.[14−17] This volume change is thermodynamically driven by a force to increase the configurational entropy (i.e., reduce the anisotropy in configuration) of the deformed networks. Lateral swelling under elongation or lateral shrinkage under compression results in a decrease in the configurational anisotropy of the distorted networks. The SR gels originally possess a unique function (pulley effect) to increase the configurational entropy of the deformed networks.[2,3] The stretching-induced swelling behavior of the SR gels is expected to differ from that of classical gels and to provide an important basis for the complete understanding of the pulley effect.

We employ three types of PR-based SR gels with various degrees of the mobility of slide-rings (CDs) as the specimens. One is a PR gel swollen by dimethyl sulfoxide, which is a good solvent for PR. The second is a water-swollen PR gel where the CD molecules form finite aggregates because of the hydrogen bonding of hydroxyl groups. The third is also a water-swollen PR gel but with modified CDs in which the hydroxyl groups are partially hydroxypropylated in order to suppress the aggregation of CDs. We compare the stretching-induced swelling behavior of these PR gels with that of chemically cross-linked gels to reveal the pulley effect that homogenizes the structure of deformed networks.

Experimental Section

Polyrotaxane (PR) Gels. Polyrotaxane composed of α-cyclodextrin (CD) and poly(ethylene glycol) (PEG) capped with 1-adamantanamine was synthesized by using a method described elsewhere.[18] The number-average molecular weight of PEG is

*To whom correspondence should be addressed. E-mail: urayama@rheogate.polym.kyoto-u.ac.jp (K.U.); kohzo@molle.k.u-tokyo.ac.jp (K.I.).

Published on Web 09/30/2009

1.15×10^5. The inclusion ratio (i.e., the filling rate of α-CD to a full filling state) for the PR was estimated to be 21% by ^{1}H NMR analysis: The PR contains ca. 280 CDs on a PEG chain composed of ca. 2600 ethylene glycol units. It is assumed here that a single α-CD molecule includes two ethylene glycol units. Hydroxypropylated polyrotaxane (H-PR) was prepared by substituting some hydroxyl groups on the α-CD molecules with hydroxypropyl groups using propylene oxide.[19,20] The average number of hydroxypropyl groups per CD molecule was evaluated to be 7.7 by ^{1}H NMR analysis.

The PR gels (PRG and H-PRG) were prepared by the intermolecular cross-linking of PR and H-PR, respectively, using 1,4-butanediol diglycidyl ether as a cross-linker. PR or H-PR was dissolved with the cross-linker in 1.5 N NaOH aqueous solution so that the concentrations of PR and the cross-linker could be 0.15 g/mL and 5 vol %, respectively. The solutions were poured into a mold. Gelation was conducted at room temperature for 20 h. The resultant gels were immersed in ion-exchanged water until the swelling attained equilibrium. The water was renewed several times in order to wash out the unreacted materials. PRG and H-PRG swollen by water were called PRG/W and H-PRG/W, respectively. The PRG swollen by dimethyl sulfoxide (DMSO) (PRG/DMSO) was made by immersing the dried PRG/W in DMSO until the equilibrium for swelling.

Polyacrylamide (PAA) and Polybutadiene (PB) Gels. Poly(acrylamide) gels (PAAGs) were prepared by the radical copolymerization of an acrylamide monomer and methylenebis(acrylamide) (cross-linker) employing ammonium persulfate as an initiator. The mixture was dissolved in water. The total reactant concentration was 10 wt %, and the molar ratio [monomer]/[cross-linker] was 200. Gelation was conducted at 5 °C for 24 h in a glass container. The resultant gel was allowed to swell in water.

Polybutadiene (BR01, JSR Corporation) was cross-linked using dicumyl peroxide. The concentration of dicumyl peroxide was 0.10 wt %. The cross-linked polybutadiene (PBG) was immersed in bis(2-ethylhexyl) adipate (DEHA) until the swelling equilibrium was attained.

The swelling solvents (water and DEHA) were renewed several times in the swelling procedures in order to extract unreacted species.

Measurements. The rectangular specimens were stretched in each solvent at 25 °C using Tensilon-RTM500 equipped with a solvent bath. Before elongation, the swelling was equilibrated in the solvent bath. The specimens were elongated at a constant cross-head speed of 100 mm/min up to the destination stretching ratio (α_x). The transverse dimensional change in the gels under a constant elongation of α_x was observed with a CCD camera. After the swelling under the elongation was equilibrated, the imposed strain was completely released. After the equilibration of swelling in the relaxed state, the specimen was stretched to the next destination of α_x. This cycle was repeated for different values α_x ranging from 1.05 to 2.0.

Theoretical Background for Stretching-Driven Swelling of Classical Gels. In this section, we provide a simple review for the theoretical background for the stretching-driven swelling of classical gels. Let us consider the imposition of a constant uniaxial elongation (α_x) to a rectangular gel that is fully swollen in solvents with a network volume fraction of ϕ_0 (Figure 1). According to the Flory−Rehner hypothesis,[21] the free energy change (ΔF) in the swelling of gels is expressed as a sum of the contributions of isotropic mixing (ΔF_{mix}) and deformation by rubber elasticity (ΔF_{el}). In the classical theory,[21,22] ΔF_{mix} and ΔF_{el} are given by the Flory−Huggins lattice model and the classical Gaussian network model, respectively:

$$\Delta F = \Delta F_{mix} + \Delta F_{el}$$

$$= N_s k_B T[\ln(1-\phi)+\chi\phi] + \frac{N_c k_B T}{2}(\lambda_x^2+\lambda_y^2+\lambda_z^2-3) \quad (1)$$

where k_B is the Boltzmann constant; T, the absolute temperature; N_s, the number of solvent molecules; N_c, the number of elastically effective network chains; and χ, the Flory−Huggins solubility parameter. The principal ratio λ_i ($i = x, y, z$) represents the deformation measured from the reference state, and λ_i is expressed by $\lambda_i = \lambda_0\alpha_i$, where λ_0 ($= \phi_0^{-1/3}$) is the isotropic expansion resulting from the free swelling. The network volume fraction ϕ in the gel is related to λ_i ($i = x, y, z$) as $\phi^{-1} = V/V_{00} = \lambda_x\lambda_y\lambda_z$, where V is the volume of the gel and the subscript 00 denotes the reference state. The true stress (force per cross section in the deformed state) in the i-direction σ_i ($i, j, k = x, y, z$) is given by

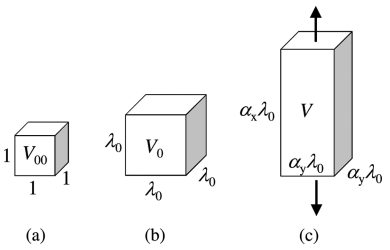

Figure 1. (a) Reference state. (b) Equilibrium swollen state with a volume of V_0. (c) Externally imposed stretching α_x in the equilibrium swollen state (b) induces further swelling ($V > V_0$).

$$\sigma_i = \frac{1}{l_j l_k}\left(\frac{\partial \Delta F}{\partial l_i}\right) = \frac{1}{V_{00}\lambda_j\lambda_k}\left(\frac{\partial \Delta F}{\partial \lambda_i}\right) \quad (2)$$

where l_i is the dimension along the i-direction in the deformed state. From eq 2, we obtain

$$\frac{\sigma_i}{k_B T} = \frac{1}{\nu_s}[\ln(1-\phi)+\phi+\chi\phi^2] + \frac{N_c}{V}\lambda_i^2$$

$$= \frac{1}{\nu_s}[\ln(1-\phi)+\phi+\chi\phi^2] + \frac{N_c\phi}{V_{00}}\left(\frac{\alpha_i}{\phi_0^{1/3}}\right)^2 \quad (3)$$

where v_s is the volume of a solvent molecule given by $v_s = (1-\phi)V/N_s$. The stresses in the y- and z-directions are zero, i.e.

$$\frac{1}{\nu_s}[\ln(1-\phi)+\phi+\chi\phi^2] + \frac{n_c\phi_0^{1/3}}{\alpha_x} = 0 \quad (4)$$

where $n_c = N_c/V_{00}$ is the number density of elastically effective network chains, and the relation $\alpha_x\alpha_y^2 = \phi_0/\phi$ is used. Equation 4 provides the condition of the equilibrium swelling under an imposed stretching of α_x. Further, the swollen state before stretching ($\phi = \phi_0$ and $\alpha_x = 1$) satisfies eq 4:

$$\frac{1}{\nu_s}[\ln(1-\phi_0)+\phi_0+\chi\phi_0^2] + n_c\phi_0^{1/3} = 0 \quad (5)$$

For highly swollen gels satisfying $\phi \ll 1$ and $\phi_0 \ll 1$, the logarithmic term in eqs 4 and 5 may be approximated as $\ln(1-x) \approx 1 - x - x^2/2$, and the relation between α_x and α_y is then obtained as

$$\alpha_y = \alpha_x^{-1/4} \quad (6)$$

Poisson's ratio (μ) for *finite* uniaxial deformation is generally defined by

$$\mu = -\frac{\varepsilon_y}{\varepsilon_x} = -\frac{\ln\alpha_y}{\ln\alpha_x} \quad (7)$$

where ε_i ($i = x, y$) is the *true* strain in the i-direction:

$$\varepsilon_i = \ln\alpha_i \quad (8)$$

Note that eq 7 using true strain is a generalized definition of Poisson′s ratio whose validity is extended to finite strain, not limited within small strain. Poisson's ratio is a measure of the

strain-induced volume change because the relative volume ratio before and after elongation is given by

$$\frac{V}{V_0} = \alpha_x \alpha_y{}^2 = \alpha_x{}^{1-2\mu} \tag{9}$$

When the stretching induces finite swelling, μ is less than 1/2. From eqs 6 and 7, the osmotic Poisson's ratio (μ_{os}) for highly swollen gels is given by

$$\mu_{os} = \frac{1}{4} \tag{10}$$

independently of α_x. The same value of μ_{os} was derived by Daoud et al.[16] and Alexander et al.[17] using a blob model for highly swollen gels under significant stretching. Geissler et al.[23] and Takigawa et al.[14] obtained similar values of μ_{os} (0.278 and 1/6, respectively) for highly swollen gels under infinitesimal deformation ($\alpha_x \approx 1$). The former used a scaling approach for good solvent systems, and the latter employed elastic energy with a logarithmic term in the early Flory theory in eq 1. The strain-induced volume change under consideration originates from solvent uptake, and as a result, the polymer concentration in gels is not constant before and after deformation. The "osmotic" Poisson′s ratio should be distinguished from the conventional Poisson′s ratio defined for deformations in air without composition change.

For modestly swollen gels in marginal solvents, μ_{os} is obtained by solving eqs 4 and 5 numerically. Some typical examples are shown in Figure 2. Importantly, μ_{os} is substantially *independent* of α_x in general cases, while μ_{os} increases slightly with a decrease in the solvent quality (i.e., χ increases).

Results and Discussion

The appearances of the three types of PR gels are shown in Figure 3. PRG/DMSO and H-PRG/W are transparent, while PRG/W is opaque. The opacity of PRG/W stems from finite aggregates of CD molecules formed because of hydrogen bonding. The transparent appearance of H-PRG/W indicates that hydroxypropylation in α-CDs considerably suppresses their aggregation. This is consistent with the fact that the hydroxypropylation of PR significantly improves the solubility of PR in aqueous solutions.[19,20] Table 1 lists the characteristics of each sample. PRG/W has a higher Young's modulus (E) and exhibits a higher ϕ_0 (i.e., lower degree of swelling) than H-PRG/W because the CD aggregates in PRG/W act as additional cross-links.[12] H-PRG/W is similar in E and ϕ_0 to PRG/DMSO. This confirms again that the CDs on the PEG chain in H-PRG/W are well dispersed because of the hydroxypropylation. In Figure 3 and Table 1, it is observed that PRG/W is thicker than the other two PR gels despite the larger ϕ_0, which is simply because each gel was separately made and had different thickness at gelation.

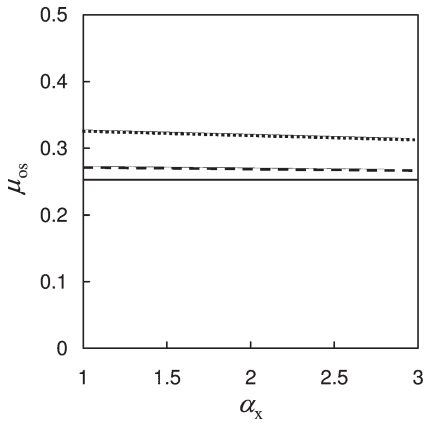

Figure 2. Dependence of osmotic Poisson's ratio (μ_{os}) on imposed elongation (α_x) predicted by the classical theory. The solid line depicts the prediction for highly swollen gels with $\phi_0 \ll 1$. The dashed and dotted lines represent the numerical results for moderately swollen gels with $\phi_0 = 0.16$ ($\chi = 0.13$) and $\phi_0 = 0.26$ ($\chi = 0.42$), respectively. In the calculations, $N_c/V_{00} = 3 \times 10^{25}$ m^{-3} and $v_s = 7 \times 10^{-28}$ m^3 are employed.

Figure 4 shows the time dependence of the transverse *true* strain (ε_y) for the PR gels under various elongations (α_x). The time $t = 0$ corresponds to the state immediately after the imposition of the elongation of interest. The time required for elongation was less than 40 s, which was negligibly short compared with the time scale of the subsequent induced swelling. The deformation at $t = 0$ was accompanied by no appreciable volume change. The Poisson's ratio at $t = 0$ (μ^0) for each gel is ca. 0.49, which is very close to 1/2 for incompressible cases: $\mu^0 = -\varepsilon_y^0/\varepsilon_x$, where ε_x and ε_y^0 are the imposed true strain ($\varepsilon_x = \ln \alpha_x$) and ε_y at $t = 0$. After the imposition of elongation ($t > 0$), finite stretching-induced swelling occurs: The lateral dimension slowly increases (i.e., $|\varepsilon_y|$ decreases) toward the new equilibrium value under elongation. The equilibrium osmotic Poisson's ratio (μ_{os}) is evaluated from ε_y in the long time limit (ε_y^∞):

$$\mu_{os} = -\frac{\varepsilon_y^\infty}{\varepsilon_x} \tag{11}$$

It should be emphasized again that the Poisson′s ratio (eqs 7 and 11) based on true strain ε (eq 8) is applicable to finite strain, not limited to infinitesimal strain.

Figure 3. Appearance of the three types of polyrotaxane gels: (left) PRG/DMSO; (middle) PRG/W; (right) H-PRG/W. PRG/DMSO and H-PRG/W are transparent, while PRG/W is opaque.

Table 1. Sample Characteristics

sample	dimensions: length × width × thickness (mm^3)	ϕ_0	E (kPa)	D (10^{-10} m^2/s)	f (10^{14} N s/m^4)
PRG/DMSO	60 × 6.0 × 3.0	0.035	2.7	2.3	0.29
H-PRG/W	60 × 8.0 × 3.0	0.032	2.6	4.5	0.14
PRG/W	60 × 8.0 × 5.0	0.083	8.2	6.7	0.33
PAAG/W	60 × 7.2 × 1.2	0.055	29	4.1	2.0
PBG/DEHA	60 × 8.0 × 2.3	0.26	200	1.1	64

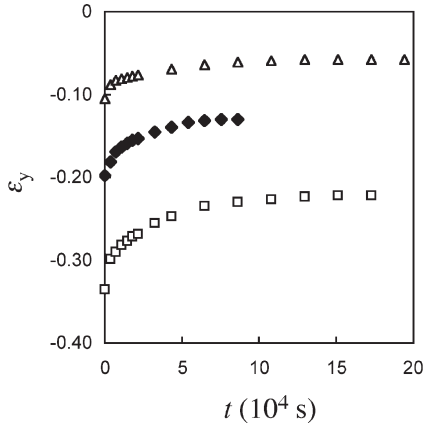

Figure 4. Time dependence of lateral true strain (ε_y) under imposed stretching (α_x). Open rectangular, filled diamond, and open triangular symbols represent the data of H-PRG/W at $\alpha_x = 2.0$, PRG/DMSO at $\alpha_x = 1.5$, and PRG/W at $\alpha_x = 1.25$, respectively.

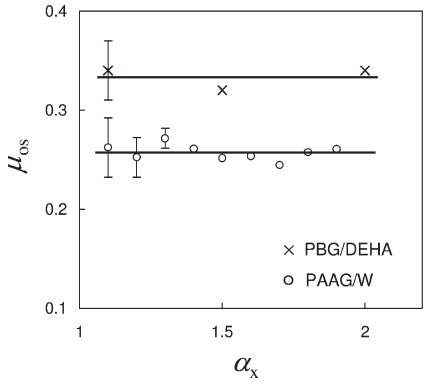

Figure 5. Dependence of osmotic Poisson's ratio (μ_{os}) on imposed stretching (α_x) for PBG/DEHA and PAAG/W.

A finite stretching-induced swelling was observed for all samples under various α_x. The α_x dependence of μ_{os} for the chemically cross-linked gels PAAG/W and PBG/DEHA is shown in Figure 5. The error bar in the figure indicates the error in the measurement of the lateral dimension. The influence of this error on μ_{os} decreases with an increase in α_x because the resultant change in the lateral dimension increases. None of the chemical gels exhibit an appreciable dependence of μ_{os} on α_x. This behavior agrees with the expectation of the classical theory shown in Figure 2. The difference in the μ_{os} of these two gels results from the difference in the degree of swelling before elongation (ϕ_0^{-1}). The value of μ_{os} ($\approx$0.26) for PAAG/W of $\phi_0 = 0.055$ is very close to the model prediction for highly swollen gels of $\phi_0 \ll 1$ ($\mu_{os} = 1/4$). PBG/DEHA with a modest degree of swelling ($\phi_0 = 0.26$) exhibits a larger μ_{os} ($\approx$0.33) than PAAG/W, which accords with the trend of the theoretical prediction (Figure 2).

Figure 6 displays the α_x dependence of μ_{os} for the three types of PR gels. The value of μ_{os} for PRG/W ($\phi_0 = 0.083$) is ca. 0.24 and is independent of α_x, which is similar to the result of the chemically cross-linked hydrogel PAAG/W with almost the same degree of swelling ($\phi_0 = 0.055$) in Figure 5. In contrast, μ_{os} for PRG/DMSO and H-PRG/W is dependent on α_x: μ_{os} increases with α_x in the region of $\alpha_x < 1.5$, whereas μ_{os} is almost constant at $\alpha_x > 1.5$. It should be emphasized that no effect of deformation hysteresis on μ_{os} was observed: These gels recovered to their original dimensions from the stretching-induced swollen states after a sufficiently long time (which is comparable to the equilibration time for the induced swelling) subsequent to the removal of the imposed strain. The second stretching of identical

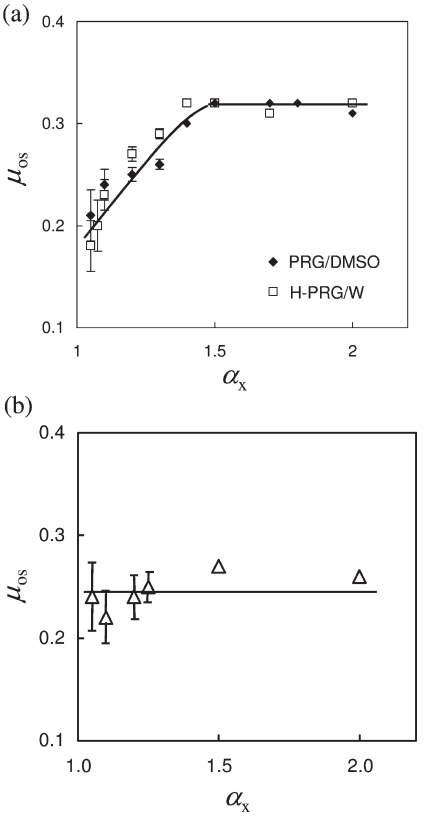

Figure 6. Dependence of osmotic Poisson's ratio (μ_{os}) on imposed stretching (α_x) for (a) PRG/DMSO, H-PRG/W, and (b) PRG/W.

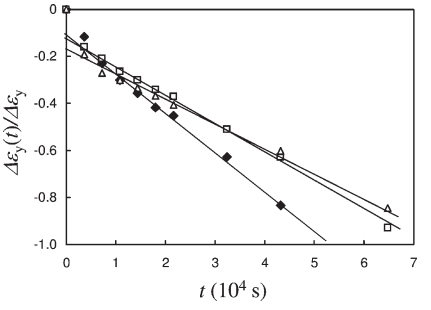

Figure 7. Semilog plot of reduced lateral strain $\Delta\varepsilon_y(t)/\Delta\varepsilon_y$ vs time for the data in Figure 4. The symbols are the same as those in Figure 4.

α_x resulted in the same value of μ_{os} as the first stretching. The marked difference in the α_x dependence of μ_{os} among the three PR gels results from the difference in the mobility of slide-rings (CDs) along the network strands. The CDs in PRG/W with an opaque appearance (Figure 3) are expected to lose or reduce the mobility considerably because of their aggregations. Therefore, PRG/W exhibits the same features as the chemically cross-linked hydrogels. The α_x-dependent μ_{os} for PRG/DMSO and H-PRG/W is a characteristic of PR gels with highly mobile slide-rings. No significant difference is observed for PRG/DMSO and H-PRG/W in the elastic and osmotic properties such as μ_{os}, E, and ϕ_0. This indicates that the elastically effective slide-rings in these two gels are almost similar in number and mobility and that the solubility of H-PR in water is comparable to that of PR in DMSO in the concentration regime of interest. The mechanism of the α_x-dependent μ_{os} for these PR gels will be discussed in a later section.

The time dependence of ε_y provides a basis for the discussion of the dynamics of the stretching-induced swelling. Figure 7 shows the semilog plots of $\Delta\varepsilon_y(t)/\Delta\varepsilon_y$ vs time for the data in Figure 3.

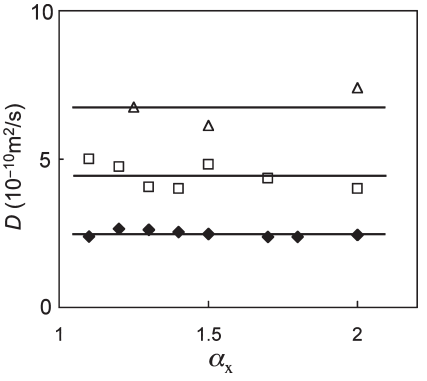

Figure 8. Dependence of diffusion constant (D) on imposed stretching (α_x) for PRG/DMSO, H-PRG/W, and PRG/W.

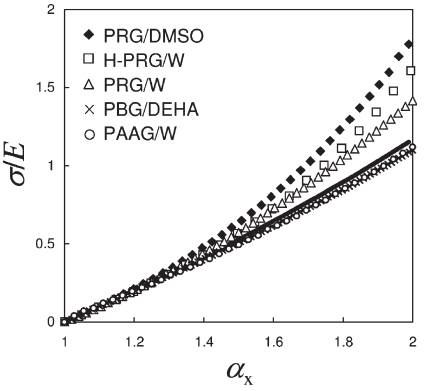

Figure 9. True stress (σ)−elongation (α_x) curve of each gel. The true stress is reduced by the initial Young's modulus (E) of each gel. The solid line represents the corresponding curve of the classical Gaussian network model.

The quantities $\Delta\varepsilon_y(t)$ and $\Delta\varepsilon_y$ are given by $\Delta\varepsilon_y(t) = \varepsilon_y - \varepsilon_y^{\infty}$ and $\Delta\varepsilon_y = \varepsilon_y^{0} - \varepsilon_y^{\infty}$, respectively. The data points for each gel fall on a straight line except in the time region close to $t = 0$. This indicates that the process of induced swelling almost obeys the single-exponential function $\Delta\varepsilon_y(t)/\Delta\varepsilon_y \approx \exp(-t/\tau_L)$. A similar kinetics was often observed for the swelling of chemical gels accompanied by a small volume change.[24] The characteristic time (τ_Λ) is evaluated from the inverse of the slope.

The diffusion coefficients for the gels (D) are obtained from τ_Λ using the relation $D = a(d_\infty^2/\tau_\Lambda)$, where a is a constant of the order of unity depending on the shape of gels and d_∞ is the thickness in the final state. Figure 8 displays D as a function of α_x for the three types of PR gels. Here, we have assumed that $a = 1$ for the sake of simplicity because the different values of a are derived by using various models.[25−28] As shown in the figure, D for each PR gel is almost independent of α_x. This indicates that the swelling dynamics is not influenced by the degree of stretching. The values of D for all gel samples are summarized in Table 1, and they are of the same order of magnitude as the reported values for several gels.[24,25] The diffusion constant D is correlated with the elastic and frictional properties as[29]

$$D = \frac{K_{os}+(4G/3)}{f} = \frac{E(2-\mu_{os})}{f(1-2\mu_{os})(1+\mu_{os})} \qquad (12)$$

where K_{os} and G are the osmotic bulk modulus and shear modulus, respectively, and f is the coefficient of the friction between the network and the solvent. The values of f calculated from eq 12 using the data of E, μ_{os}, and D are tabulated in Table 1. The values of μ_{os} in the small strain limit were employed in the calculation for PRG/DMSO and H-PRG/W because E in eq 12 is the modulus at small strains. The difference in f between PRG/DMSO and H-PRG/W is primarily attributed to the difference in solvent viscosity (η) affecting f as $f \sim \eta$ because they are almost similar in μ_{os}, E, ϕ_0, and network structures. In fact, the ratio of f of these two gels (ca. 2.0) accords with the ratio of η of DMSO and water (η_{DMSO} = 1.98 mPa s and η_{water} = 1.00 mPa s at 25 °C). The large f value of PBG/DEHA is mainly explained by the same reason, i.e., the high solvent viscosity (η_{DEHA} = 11.4 mPa s). In comparison, between the hydrogels where solvent viscosity effect is excluded, f of the PR hydrogels ($\sim 10^{13}$ N s/m^4) is 1 order of magnitude smaller than that of PAAG/W ($f = 2.0 \times 10^{14}$ N s/m^4). All the reported f values for the highly swollen hydrogels of polyacrylamide,[30−32] poly(*N*-isopropylacrylamide),[33] and poly(vinyl alcohol)[34,35] are of the order of 10^{14} N s/m^4 similarly to the data of PAAG/W. However, it should be noted that the moduli of the PR hydrogels ($\sim 10^3$ Pa) are 1 order of magnitude smaller than those of PAAG/W and the hydrogels used in the literatures[30−35] ($\sim 10^4$ Pa). For strict comparison, we need the f values of the hydrogels of PR and various polymers with same magnitude of elastic modulus, but this is beyond the scope of present paper.

The diffusion constant D reflects the slow diffusion of the gels during swelling. It is not directly related to the movement of slide-rings in response to the imposed deformation. A quasi-elastic light scattering study[36] showed that the time scale of the sliding mode of the CDs along PEG chains was of the order of 10^{-2} s, which is markedly fast compared with the time scale of swelling. In addition, we observed no appreciable stress relaxation at constant α_x for PRG/DMSO in air. This indicates the fast equilibration of the displacement of slide-rings in response to the imposed deformation.

Here, we consider the mechanism of the α_x-dependent μ_{os} for PRG/DMSO and H-PRG/W, i.e., the PR gels with highly mobile slide-rings. As long as the imposed elongation remains moderate, the slide-rings are highly mobile (i.e., the pulley effect is active). As the elongation increases, the slide-rings move to the ends of the network strands. In the extensively stretched state, many slide-rings are highly localized and stacked to the chain ends and loose their mobility. The PR gels in such a highly stretched state are expected to behave in qualitatively the same manner as the gels with fixed cross-links. The level-off of μ_{os} in the regime of $\lambda_x > 1.5$ is an indication of the suppression of the movement of slide-rings because of significant elongation. The suppression effect of the movement of slide-rings is also recognizable in the stress−strain relations of these PR gels. Figure 9 shows the λ_x dependence of true stress (σ) for each gel in air. In the figure, σ is reduced by the Young's modulus (E) of each sample in order to focus on the λ_x dependence of σ. The prediction of the classical Gaussian network model is also shown in the figure: $\sigma/E = (\lambda_x^2 - \lambda_x^{-1})/3$. The results of the chemically cross-linked gels obey the model prediction, in accordance with many earlier observations for the uniaxial stretching of the elastomers in the fully swollen states.[22,37] In contrast, a definite upward deviation from the theoretical curve is observed for PRG/DMSO and H-PRG/W in the regime of $\lambda_x > 1.5$. This upturn of stress is expected to originate from the high localization of the slide-rings at the chain ends, which leads to the full stretch effect of the network strands with finite chain lengths.[38] The plateau values of μ_{os} (≈ 0.32) at high stretching where the pulley effect is suppressed are appreciably higher than μ_{os} (≈ 0.25) of the chemical gel PAAG/W with the similar polymer concentration. This is expected to result from the difference in the nonlinear stress−strain behavior between the PR gels and PAAG/W because the nonlinear elastic properties influence the swelling equilibrium under high elongation.

Slide-rings possess high mobility in the modest stretching of $\lambda_x < 1.5$, where μ_{os} is α_x-dependent. A major origin of stretching-driven swelling is an entropic force to decrease the configurational

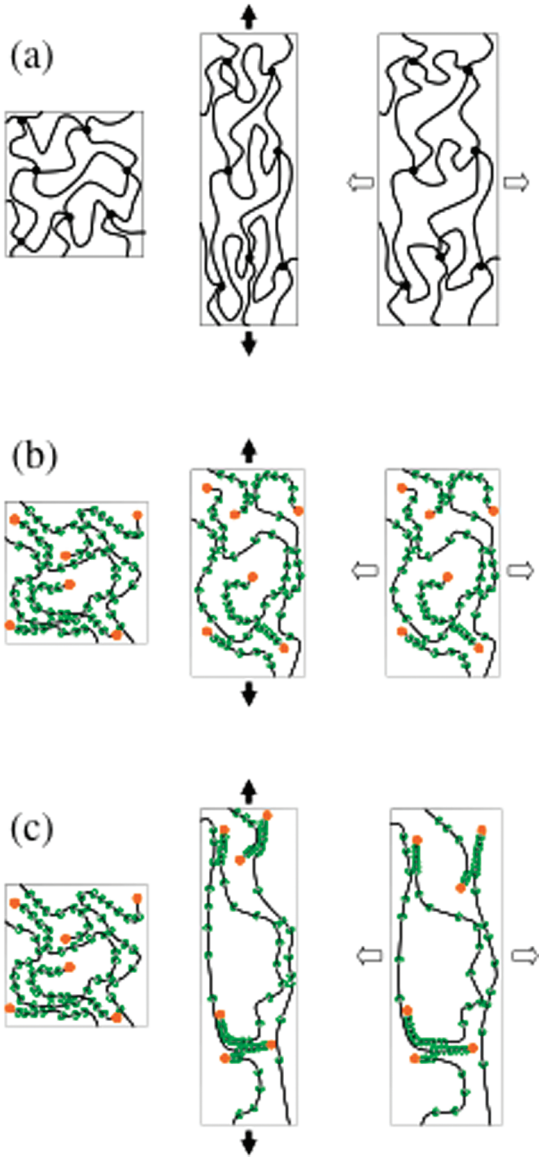

Figure 10. Stretching-induced swelling of (a) classical gels with topologically fixed cross-links, (b) slide-ring gels under moderate stretching, and (c) slide-ring gels under large stretching: (left column) undeformed state; (middle column) just after the imposition of a constant stretching; (right column) induced lateral swelling.

anisotropy of the networks caused by the imposed elongation (Figure 10a). The PR gels with highly mobile slide-rings originally possess the pulley effect to homogenize the network topology under applied strain. Therefore, the PR gels with the pulley effect are capable of reducing the configurational anisotropy of the stretched networks prior to the stretching-induced swelling (Figure 10b). The pulley effect significantly suppresses the subsequent induced swelling, which results in an increase in μ_{os}. If the slide-rings were immobile, μ_{os} would remain ca. 0.20 (corresponding to μ_{os} in the small strain limit) irrespective of the stretching. The α_x-dependent μ_{os} observed macroscopically is qualitatively consistent with the features of the microscopic structure revealed by a small-angle X-ray scattering study[5] on a DMSO-swollen PR gel. That is, finite stretching causes no significant anisotropy in the network configuration.

The α_x-dependent μ_{os} is expected to originate from the unique elastic energy (F_{el} in eq 1) of the PR gels with the pulley effect. The detailed characterization of the finite deformation behavior of the PR gels is required for elucidating the form of F_{el}. Further, several molecular parameters such as the concentration of slide-rings and the length of network strands are expected to significantly influence the α_x dependence of μ_{os}. These issues will be investigated in our future study.

Summary

The osmotic Poisson's ratio of the PR gels with highly mobile slide-rings (DMSO-swollen PR gels and water-swollen hydroxypropylated PR gels) is dependent on the imposed stretching (α_x): μ_{os} increases with α_x in the case of moderate stretching, whereas it is constant in the case of high stretching. This α_x-dependent μ_{os} is in contrast to the α_x-independent μ_{os} of the classical gels with fixed cross-links and the water-swollen PR gels with constrained slide-rings. An increase in μ_{os} due to elongation results from the molecular pulley effect of the movable cross-links that homogenizes the configuration the deformed networks prior to the stretching-driven swelling. The pulley effect significantly suppresses the subsequent stretching-induced swelling that originates from an entropic force to decrease the configurational anisotropy in the deformed networks. In the case of significant elongation, μ_{os} becomes independent of α_x as in the case of classical gels with fixed cross-links. This is because the significant elongation causes a considerable localization and stacking of many slide-rings to the chain ends, which results in the loss or considerable suppression of the mobility of the slide-rings.

Acknowledgment. The authors thank Dr. Shoji Nosaka for his assistance in tensile experiments. This work was partly supported by a Grant-in-Aid for Scientific Research (S) (No. 20221005) and a Grant-in-Aid on Priority Area "Soft Matter Physics" (No. 21015014) from the Ministry of Education, Culture, Sports, Science and Technology (MEXT), Japan.

References and Notes

(1) Granick, S.; Rubinstein, M. *Nat. Mater.* **2004**, *3*, 586–587.
(2) Ito, K. *Polym. J.* **2007**, *39*, 489–499.
(3) Okumura, Y.; Ito, K. *Adv. Mater.* **2001**, *13*, 485–487.
(4) Karino, T.; Okumura, Y.; Zhao, C. M.; Kataoka, T.; Ito, K.; Shibayama, M. *Macromolecules* **2005**, *38*, 6161–6167.
(5) Shinohara, Y.; Kayashima, K.; Okumura, Y.; Zhao, C. M.; Ito, K.; Amemiya, Y. *Macromolecules* **2006**, *39*, 7386–7391.
(6) Mendes, E.; Lindner, P.; Buzier, M.; Boue, F.; Bastide, J. *Phys. Rev. Lett.* **1991**, *66*, 1595–1598.
(7) Ramzi, A.; Zielinski, F.; Bastide, J.; Boue, F. *Macromolecules* **1995**, *28*, 3570–3587.
(8) Rouf, C.; Bastide, J.; Pujol, J. M.; Schosseler, F.; Munch, J. P. *Phys. Rev. Lett.* **1994**, *73*, 830–833.
(9) Bastide, J.; Leibler, L. *Macromolecules* **1988**, *21*, 2647–1649.
(10) Panyukov, S.; Rabin, Y. *Macromolecules* **1996**, *29*, 7960–7975.
(11) Fleury, G.; Schlatter, G.; Brochon, C.; Hadziioannou, G. *Polymer* **2005**, *46*, 8494–8501.
(12) Samitsu, S.; Araki, J.; Kataoka, T.; Ito, K. *J. Polym. Sci., Part B: Polym. Phys.* **2006**, *44*, 1985–1994.
(13) Chiarelli, P.; Basser, P. J.; Derossi, D.; Goldstein, S. *Biorheology* **1992**, *29*, 383–398.
(14) Takigawa, T.; Urayama, K.; Morino, Y.; Masuda, T. *Polym. J.* **1993**, *25*, 929–937.
(15) Hecht, A. M.; Horkay, F.; Geissler, E.; Zrinyi, M. *Polym. Commun.* **1990**, *31*, 53–55.
(16) Daoud, M.; de Gennes, P. G. *J. Phys.* (*Paris*) **1977**, *38*, 85–93.
(17) Alexander, S.; Rabin, Y. *J. Phys.: Condens. Matter* **1990**, *2*, Sa313–Sa315.
(18) Araki, J.; Zhao, C. M.; Ito, K. *Macromolecules* **2005**, *38*, 7524–7527.
(19) Araki, J.; Ito, K. *J. Polym. Sci., Polym. Chem.* **2006**, *44*, 6312–6323.
(20) Ooya, T.; Yui, N. *Macromol. Chem. Phys.* **1998**, *199*, 2311–2320.
(21) Flory, P. J.; Rehner, J. *J. Chem. Phys.* **1943**, *11*, 521–526.
(22) Treloar, L. R. G. *The Physics of Rubber Elasticity*, 3rd ed.; Clarendon Press: Oxford, 1975.
(23) Geissler, E.; Hecht, A. M.; Horkay, F.; Zrinyi, M. *Macromolecules* **1988**, *21*, 2594–2599.

(24) Tanaka, T.; Fillmore, D. J. *J. Chem. Phys.* **1979**, *70*, 1214–1218.
(25) Li, Y.; Tanaka, Y. *J. Chem. Phys.* **1990**, *92*, 1365–1371.
(26) Wang, C.; Li, Y.; Hu, Z. *Macromolecules* **1997**, *30*, 4727–4732.
(27) Yamaue, T.; Doi, M. *J. Chem. Phys.* **2005**, *122*, 084703.
(28) Urayama, K.; Murata, N.; Nosaka, S.; Kojima, M.; Takigawa, T. *Prog. Colloid Polym. Sci.* **2009**, *136*, in press.
(29) Tanaka, T.; Hocker, L. O.; Benedek, G. B. *J. Chem. Phys.* **1973**, *59*, 5151–5159.
(30) Tokita, M.; Tanaka, T. *J. Chem. Phys.* **1991**, *95*, 4613–4621.
(31) Urayama, K.; Okada, S.; Nosaka, S.; Watanabe, H.; Takigawa, T. *J. Chem. Phys.* **2005**, *122*, 024906.
(32) Suzuki, Y. Y.; Tokita, M.; Mukai, S. *Eur. Phys. J. E*, Web-released.
(33) Nosaka, S.; Ishida, T.; Urayama, K.; Takigawa, T. *J. Membr. Sci.* **2007**, *305*, 325–331.
(34) Takigawa, T.; Uchida, K.; Takahashi, K.; Masuda, T. *J. Chem. Phys.* **1999**, *111*, 2295–2300.
(35) Nosaka, S.; Okada, S.; Takayama, Y.; Urayama, K.; Watanabe, H.; Takigawa, T. *Polymer* **2005**, *46*, 12607–12611.
(36) Zhao, C. M.; Domon, Y.; Okumura, Y.; Okabe, S.; Shibayama, M.; Ito, K. *J. Phys.: Condens. Matter* **2005**, *17*, S2841–S2846.
(37) Gumbrell, S. M.; Mullins, L.; Rivlin, R. S. *Trans. Faraday Soc.* **1953**, *49*, 1495.
(38) Koga, T.; Tanaka, F. *Eur. Phys. J. E* **2005**, *17*, 225–229.